

UNCLASSIFIED

AD NUMBER
ADB222555
NEW LIMITATION CHANGE
TO Approved for public release, distribution unlimited
FROM Distribution authorized to DoD only. Other requests shall be referred to Embassy of Australia, Attn: Joan Bliss, Head. Pub. Sec. -Def/Sci, 1601 Massachusetts Ave., NW, Washington, DC 20036.
AUTHORITY
DSTO ltr dtd 27 Jan 2000

THIS PAGE IS UNCLASSIFIED

O

AR-008-530

DSTO-TR-0156

T

Optical Propagation Effects of an Underwater Laser Range-gated Imaging System

B.W. Koerber, T. Adams and P.J. Wilsen

S

Officers of the Defence Communities of Australia, UK, USA, Canada & NZ may have access to this document. Others refer to Document Exchange Centre, CP2-5-08, Campbell Park Offices, CANBERRA ACT 2600 AUSTRALIA

DTC QUALITY INSPECTED 4

19970422 069

I

DEPARTMENT OF DEFENCE
DEFENCE SCIENCE AND TECHNOLOGY ORGANISATION

~~DISTRIBUTION STATEMENT B: Distribution authorized to DoD Components only
. Other requests shall be referred to~~

Embassy of Australia
Attn: Joan Bliss
Head. Pub. Sec.-Def/Sci.
1601 Massachusetts Ave., NW
Washington, DC 20036

~~Embassy of Australia~~

Optical Propagation Effects of an Underwater Laser Range-gated Imaging System

B.W. Koerber, T. Adams and P. J. Wilsen

**Land, Space and Optoelectronics Division
Electronics and Surveillance Research Laboratory**

DSTO-TR-0156

ABSTRACT

A report on the verification of a suite of mathematical models related to propagation of light in water. The developed models were assessed by comparison with experimental results for forward scattering and backscattering, in addition to image propagation, using the high performance underwater imaging system.

~~RELEASE LIMITATION~~

~~*Distribution additional to the initial list is limited to qualified officers of the Defence Department and the Defence Community of Australia, UK, USA, Canada and New Zealand. Other requests should be referred to Chief, Land, Space and Optoelectronics Division Electronics and Surveillance Research Laboratory.*~~

~~DEPARTMENT OF DEFENCE~~

~~DEFENCE SCIENCE AND TECHNOLOGY ORGANISATION~~

Published by

*DSTO Electronics and Surveillance Research Laboratory
PO Box 1500
Salisbury, South Australia, Australia 5108*

Telephone: (08) 8259-5555

Fax: (08) 8259-5055

© Commonwealth of Australia 1996

AR-008-530

May 1996

Conditions of Release and Disposal

1. *This document is the property of the Australian Government; the information it contains is released for defence purposes only and must not be disseminated beyond the stated distribution without prior approval.*
2. *The document and the information it contains must be handled in accordance with security regulations applying in the country of lodgement, downgrading instructions must be observed and delimitation is only with the specific approval of the Releasing Authority as given in the Secondary Distribution statement.*
3. *This information may be subject to privately owned rights.*
4. *The officer in possession of this document is responsible for its safe custody. When no longer required this document should be destroyed and the notification sent to: Senior Librarian, Defence Science and Technology Organisation, Electronics and Surveillance Research Laboratory*

Optical Propagation Effects of an Underwater Laser Range-gated Imaging System

EXECUTIVE SUMMARY

As part of a program of work to evaluate the performance of the High performance UnderWater Imaging (HUWI) system, a suite of propagation models was developed by the Land Space and Optoelectronics Division of DSTO. The objective was to develop a modelling capability that could be used to predict the performance of any underwater imaging system given a knowledge of the system and critical parameters associated with the operating environment. Models were developed to address the propagation of light from the illuminating source to the scene, propagation of light back to the imaging receiver and the quality of the image arriving at the imaging receiver. Comparison of the models with performance of the HUWI imaging system demonstrated the validity of the modelling technique.

Authors

T. Adams

Land, Space and Optoelectronics Division

The author graduated from the University of South Australia with a degree in Electronic Engineering. He has been involved with the research and development aspects of optoelectronic systems for a number of Defence related programs. His experience includes visible and infrared systems for use in airborne, maritime surface and sub-surface applications.

P.J. Wilsen

Land, Space and Optoelectronics Division

The author graduated from Adelaide University in Mathematics and Physics. He has been involved in a range of programs in the infrared and optical area. recently the author has explored the theoretical effects of image propagation and undertaken measurement of light fields using specially constructed equipment.

B.W. Koerber

Land, Space and Optoelectronics Division

The author has worked for DSTO since 1955. His experience has included optical propagation effects for the Laser Airborne Depth Sounder program (LADS). In addition to mathematical modelling of both atmospheric and underwater light propagation, the author has been the principal in an experimental program to measure water optical properties including the design and utilisation of absorption, scattering and transmittance monitors.

Contents

1. INTRODUCTION	1
2. DESCRIPTION OF HUWI.....	1
3. MONTE CARLO MODELS	2
3.1 General.....	2
3.2 Standard Monte Carlo Model	2
3.3 Limit of applicability of the standard model	3
3.4 Semi-analytic Monte Carlo model.....	3
4. MODEL VALIDATION	4
4.1 The Radiometric Equipment	4
4.2 Radiometer Calibration.....	5
4.3 The Radiometric Experiment	5
4.4 The Radiometric Measurements.....	5
5. OPTICAL PROPERTIES OF WATER	6
6. COMPARISON OF EXPERIMENTAL RESULTS WITH MODEL PREDICTIONS.....	6
6.1 Radiometer Calibration.....	6
6.2 Comparison of results for radiometers 1 and 2	6
6.3 Comparison of Results for radiometer 3	7
7. MODEL PREDICTIONS FOR HUWI.....	7
7.1 HUWI Set-to-work	8
8. CONCLUSIONS.....	8
9. REFERENCES	9
Figure 1: Volume Scattering function.....	10
Figure 2: Radiometer 1 at 0 degrees Transmitter Narrow FOV	10
Figure 3: Radiometer 1 at 40 degrees Transmitter Narrow FOV	11
Figure 4: Radiometer 1 at 0 degrees Transmitter Wide FOV.....	11
Figure 5: Radiometer 1 at 40 degrees Transmitter Wide FOV.....	12
Figure 6: Radiometer 2 at 0 degrees Transmitter Narrow FOV	12
Figure 7: Radiometer 2 at 40 degrees Transmitter Narrow FOV	13
Figure 8: Radiometer 2 at 0 degrees Transmitter Wide FOV.....	13
Figure 9: Radiometer 2 at 40 degrees Transmitter Wide FOV.....	14
Figure 10: Radiometer 3 Target Range 8.5 metres.....	14
Figure 11: Target and backscatter signals for $c=0.6 \text{ m}^{-1}$ seen by HUWI.....	15

1. Introduction

The performance of an underwater imaging system is to a large extent determined by the optical characteristics of the water in which it operates. This is particularly true where artificial illumination is required. In predicting the performance of imaging systems an understanding of the mechanisms which affect light propagation in water is vital. Because multiple scattering effects greatly complicate the propagation process, simple analytic techniques fail to provide satisfactory solutions and a combination of analytic and statistical methods is required. As part of a program of work to evaluate the performance of an active underwater range-gated imaging system (HUWI), a suite of propagation models was developed by Land Space and Optoelectronics Division of DSTO. The objective was to develop a modelling capability that could be used to predict the performance of any underwater imaging system, given a knowledge of the system and critical parameters associated with the operating environment. Models were developed to address three prime areas.

- a) The propagation of light from the illuminating source to the scene.
- b) The propagation of light back to the imaging receiver (this includes both reflected light from the scene and backscattered light from particles in the water).
- c) The quality of the image arriving at the imaging receiver.

An important aspect of the program of work was model validation. Field experiments were conducted in a large water tank to provide measured radiometric data for comparison with model predictions. This paper presents the results of that comparison.

2. Description of HUWI

The system under study is a range-gated imaging receiver coupled to a high peak power, pulsed laser for scene illumination. The imaging receiver comprises a gated image intensifier, fibre optically coupled to an asynchronous CCD camera. The laser is a frequency doubled YAG operating at 5 Hz, delivering 50 to 150 mJ of 532 nm radiation in a pulse 10 ns wide. All critical system timing is derived directly from the output of light from the laser to achieve the levels of timing stability required. The system is configured as an experimental apparatus with full control over the system exercised from a personal computer that is physically separated from the housing containing the wet system components. The fields of view of both transmitter and receiver are slaved and are variable in the range 5 to 15 degrees. Details of the range-gated imaging system are contained in the report at reference 1.

For much of the experimental work associated with model validation, the HUWI system was used primarily as a source of pulsed 532 nm radiation to permit propagation measurements to be made in a large body of water.

3. Monte Carlo Models

3.1 General

The propagation of light in water is complicated greatly by multiple scattering effects. Mathematical modelling of this process has been developed using a variety of approaches, with various degrees of success. The Monte Carlo technique was shown to be an adequate modelling method in a previous study of laser light propagation conducted in sea water at Jervis Bay (reference 2). The Monte Carlo model developed for that experiment has been modified appropriately to create additional versions which provide basic information required in the present study of image propagation in water.

3.2 Standard Monte Carlo Model

The standard Monte Carlo model simulates the passage in water of individual photons from the transmitted beam through a series of scattering events. For each segment of the three dimensional photon trajectory, values of the distance travelled before scattering and the subsequent scattering angles are determined by making random selections from appropriate cumulative probability data for these parameters. Random numbers required for this procedure are generated by the computer. Weighting factors are computed for each photon trajectory to account for the absorption losses along that path (the photon can be conceived of as a large packet of individual photons travelling in the same direction along the trajectory with individual photons being absorbed at various points along that path). Transit times through the water are computed for each photon path. After the computations have been repeated for a large number of photons, a space-time map is built up of the distribution of light flux in the water.

The magnitude of chance variations in the results ("noise") due to the random Monte Carlo process is reduced by increasing the total number of computed photon trajectories. A considerable improvement is obtained by taking advantage of the symmetry of scattering around the light beam. This gain is accomplished by combining photons that pass through specified portions of an annular region on a surface centred on the axis of the transmitter beam. Each incident photon is weighted appropriately to allow for the magnitude of the area of the particular annulus in which the photon is collected.

The standard Monte Carlo model is very suitable for computations of light flux received at the opposite end of a one-way path from a light source as a high density of photons is achieved. Thus for the study of the performance of the range-gated imaging system HUWI, the standard model is used to compute values of the distribution of the light flux at the target plane. Circular symmetry is assumed about the axis of the transmitter beam and photons are collected in annular regions. Similarly, the standard model is used to compute values of the impulse response function over various ranges from the object plane by again using circular symmetry about the beam (in this case the beam is an impulse).

3.3 Limit of applicability of the standard model

There is also a requirement to use Monte Carlo modelling methods to compute the envelope of back-scatter and target reflected signals at the receiver of the range-gated imaging system. The standard Monte Carlo model is a purely statistical computation of an ensemble of photon trajectories through the medium, with the length and direction of each trajectory segment obtained from random selections made from the relevant probability functions applying for the medium. Results are produced by accepting only those photons which are collected within the defined receiver aperture area and within the specified field of view. For the receiver of the range-gated imaging system, the geometric constraints are very restrictive, resulting in a very small probability of success for any given photon trajectory. To use the standard Monte Carlo model, it is necessary to compute a very large number of photon trajectories and to relax the geometric constraints on the receiver to provide a much larger collecting area and a much wider field of view. It was found that the latter procedure produced large errors in the computed magnitude and shape of the back-scatter and target reflected signals. Thus, it was decided to use a semi-analytic model (reference 3) to conduct this aspect of the modelling study, since the semi-analytic method offers an effective means for modelling with realistic geometric constraints and hence should provide the required accuracy in the results.

3.4 Semi-analytic Monte Carlo model

The semi-analytic Monte Carlo model uses a combination of statistical and analytic techniques to determine the receiver signal. The photon is conceived of as a large packet of identical photons travelling along the same path through water. Segments of the photon trajectory are computed using the standard Monte Carlo method. When a segment terminates at a point within the volume enclosed by the field of view of the receiver, the probability is computed of the fraction of photons that would be redirected towards the receiver. The received signal is increased by an amount representing the proportion of the photons arriving at the receiver without further attenuation.

The estimated proportion of photons collected by the receiver is given by

$$S = p(\theta) \cdot d\omega \cdot e^{-cr} \quad (1)$$

where $p(\theta)$ is the scattering phase function at angle θ

θ is the angle between the photon trajectory segment and the receiver direction (see figure 1),

$d\omega$ is the solid angle subtended by the receiver aperture

c is the attenuation coefficient

and r is the distance to the receiver.

The phase function is

$$p(\theta) = \frac{\beta(\theta)}{b} \quad (2)$$

where $\beta(\theta)$ is the volume scattering function and b is the scattering coefficient.

Since

$$\int_0^{4\pi} \beta(\theta) d\omega = b \quad (3)$$

it follows that

$$\int_0^{4\pi} p(\theta) d\omega = 1 \quad (4)$$

and hence $p(\theta)d\omega$ is the correctly scaled probability of a photon scattering in the direction of the receiver.

When each scattering event occurs within the field of view of the receiver, the value S is added to the receiver signal, and the weighting factor of the packet of photons is reduced by the value $p(\theta)d\omega$. The remaining photon packet then proceeds to the next scattering point which is computed using the standard Monte Carlo model.

4. Model Validation

An experiment was undertaken in a large fresh water tank to provide experimental radiometric data for comparison with the output from the Monte Carlo models. The experiment involved mounting the HUWI imaging equipment at one end of the water tank and deploying three purpose built radiometers in the tank. Measurements were made of the radiance and irradiance fields in the water body. The total attenuation coefficient and the absorption coefficient of the water were measured.

4.1 The Radiometric Equipment

A set of three radiometers was developed to measure radiance and irradiance fields produced by the laser beam. Each radiometer comprises a fast 10 stage photomultiplier (EMI type 9893B/350) with associated electronics coupled to a suitable lens system and mounted in a water tight housing. The output of the radiometers is buffered and fed via coaxial cable to a monitoring point where a fast digitising oscilloscope coupled to a personal computer was used to view and record the output waveforms. The EHT supply voltage for the radiometers was manually controlled by the operator to maintain an undistorted signal. The pulse width, pulse height or the entire waveform can be selectively logged to computer disk.

Two of the radiometers have narrow fields of view and provide a measure of radiance. The third has a wide field of view and provides a measure of irradiance.

4.2 Radiometer Calibration

The response of each radiometer was calibrated with all optical components in place using a frequency doubled YAG laser chopped at 800 Hz. The irradiance at the input aperture was measured with a Newport Picowatt meter and optical neutral density filters were used to attenuate the beam during the calibration procedure. Calibration data for the radiometers were used to convert the recorded signal amplitudes and EHT settings to values of irradiance for radiometer 1 and to values of radiance for radiometers 2 and 3.

4.3 The Radiometric Experiment

The radiometric measurements were made in a large sedimentation tank at a local water filtration plant. The tank dimensions of 40 m (width) x 120 m (length) x 6 m (depth) were sufficient to preclude unwanted reflections from the tank walls impacting on the radiometric measurements. The HUWI imaging equipment was deployed from an adjustable frame secured at one end of the tank at a depth of 3 m. Imaging targets and radiometers 1 and 2 were deployed from a travelling bridge structure, which was positioned at various distances from the laser source (HUWI). Radiometers 1 and 2 provided irradiance and radiance measurements of the beam as it propagated down the tank toward the target. Radiometers 1 and 2 were rotated to provide data at various angles of inclination relative to the propagating beam.

Radiometer 3 was mounted adjacent to the HUWI equipment, providing a measure of the signal envelope as seen by the imaging receiver in HUWI. This envelope comprised the combined effects of light backscattered from particles in the water and the light reflected from the imaging target.

4.4 The Radiometric Measurements

For the radiometric measurements, the HUWI laser was operated with an output of 90 mJ and a transmitter field of view of 5 and 15 degrees. The irradiance and radiance fields were measured using radiometers 1 and 2 over the range 10 to 25 m from the laser source. At each range, the transmitter field of view was set to 5 and 15 degrees and the angle of inclination of each radiometer varied between +/-40 degrees with respect to the oncoming beam.

The measurements with radiometer 3 were made at a shorter range with an imaging target suspended in the HUWI field of view. The imaging target comprised a 1.2 m x 1.2 m panel with black bars on a white background. The imaging target and HUWI field of view were aligned at a range of 8.5 m using the system as a range-gated imager. It should be noted that the measured total attenuation coefficient of the water was 0.7 and that recognisable images were obtained out to a range of 9 m. This equates to imaging performance at 6.3 attenuation lengths. The imaging performance of the HUWI system is addressed at reference 4.

All measurements were made in the same body of water. Water quality was constantly monitored for total attenuation coefficient and absorption coefficient. It was not possible to control or vary the characteristics of the water in this tank.

5. Optical Properties of Water

The optical properties of water are adequately described by the volume scattering function and the absorption coefficient. For this series of experiments only a single laser wavelength was used requiring the properties to be defined at only one wavelength.

The volume scattering function $\beta(\theta)$ as mentioned in section 3 is the differential scattering of light into a solid angle

$$ds = dv \cdot d\omega \cdot \beta(\theta) \quad (5)$$

where ds the light from the unit beam scattered in
 dv the infinitesimal volume into
 $d\omega$ the infinitesimal solid angle oriented at
 θ scatter angle relative to the direction of propagation of the beam

There is evidence that the angle dependency of the volume scattering function, (the phase function referred to in section 3) is constant for most forms of organic scattering particles (reference 5). The practical difficulties of carrying out direct measurements of the volume scattering function are so considerable (references 5,6) that it has been done infrequently and was not possible in the sedimentation tank.

When a functional form of the phase function is assumed (figure 1 shows a typical form), a measure of total scatter and absorption is sufficient to define the volume scattering function in addition to the absorption. A measure of the total scatter was obtained by measuring the total attenuation coefficient for a narrow beam and subtracting simultaneously measured values of absorption coefficient.

6. Comparison of Experimental Results with Model Predictions

6.1 Radiometer Calibration

Radiometer measurements made in the sedimentation tank were reduced using calibration data for the radiometers obtained from laboratory measurements. Recorded signal amplitudes and EHT settings were converted to values of irradiance for radiometer 1 and to values of radiance for radiometers 2 and 3.

6.2 Comparison of results for radiometers 1 and 2

The standard Monte Carlo model was used for the calculation of predicted irradiance and radiance at radiometers 1 and 2 for specified ranges from the HUWI laser transmitter and for specified orientations of the radiometer field of view. The calculations were performed for the values of attenuation and absorption coefficient measured during the experiment (see section 5).

The results of the comparison of the experimental radiometric data and the predicted results from the standard Monte Carlo model are shown in figures 2,3,4 and 5 for radiometer 1 and the narrow and wide transmitter beam widths respectively.

Figures 6,7 and 8,9 show the corresponding results for radiometer 2.

Generally the results of the comparison for radiometers 1 and 2 show good agreement. At a range of 10 metres, the measured values for radiometer 1 are lower than expected, not conforming with the trend shown in the data at higher ranges. The results for radiometer 2 show somewhat greater divergence at high ranges.

6.3 Comparison of Results for radiometer 3

The semi-analytic model was used to calculate predicted radiance at radiometer 3 located alongside the HUWI equipment. The envelope of radiance versus time was calculated to provide values of backscatter from the laser transmitter beam and the value of reflected signal from the target at a specified range. The measured values of attenuation and absorption coefficients were again used for these calculations.

The results of the comparison of radiometer 3 measurements and the semi-analytic Monte Carlo model predictions are shown in figure 10 for a target range of 8.5 metres from the laser transmitter. Good agreement is shown in the magnitude of the peaks of the measured and modelled backscatter signals and also in the peaks of the measured and modelled target reflected signals. A small discrepancy can be seen in the width of the envelope of the backscatter signal.

Results of the comparison of radiometer 3 measurements and model predictions at shorter ranges are not shown in this report due to large discrepancies in the magnitude of the compared target signals. It is thought that the good agreement at 8.5 metres was due to the fact that the target was aligned for the highest signal at this range, but the poor agreement at shorter ranges occurred because of decreasing overlap of the fields of view as the range decreased.

7. Model Predictions for HUWI

All of the preceding model calculations have been specific to the requirement of the experiment. The validation work involved exercising the models using input data specific to the tank experiment. Input parameters were derived from the measured optical characteristics of the water, from the physical characteristics of the laser and radiometers, and from the geometric constraints of the experiment. The model results were then compared with data measured experimentally to establish confidence in the modelling process.

Model predictions have been instrumental in the set-to-work of the HUWI equipment. The plot in figure 11 shows a typical target and backscatter envelope determined for the HUWI system in its current configuration, with a target at 10 m range (90 nS after laser fire). Figure 10 is representative of the signal envelope for the

experimental configuration with the target at a range of 8.5 m in water with a total attenuation coefficient of 0.7. The "noise spikes" evident on both plots are a result of the semi-analytic Monte Carlo technique employed in the model (reference 3 for further details). Note the much higher backscatter levels experienced by the imaging receiver in HUWI (3 orders of magnitude). This effect is due to the geometry of the HUWI equipment which results in a much larger common volume being shared by the laser and imaging receiver.

7.1 HUWI Set-to-work

Model predictions of target and backscatter signals for HUWI were used in a number of laboratory experiments to establish range-gated system operation. Experiments were conducted using a small, 532 nm pulsed laser in combination with optical components, neutral density filters and fibre optic delay lines to simulate realistic backscatter and target signals.

The sensitivity of the HUWI imaging receiver in the gated mode was measured and full range-gated system functionality established using the simulated signals in air. Imaging receiver sensitivity was found to be consistent with that determined theoretically for the system when operated in the gated mode.

Experiments were also conducted to investigate the effect of flooding the imaging receiver with high light levels prior to receipt of the much lower target return signal; conditions consistent with those encountered in turbid water. Concerns over a possible reduction in receiver sensitivity, due to space charge effects associated with the image intensifier photo-cathode, were found to be groundless. No degradation in imaging sensitivity was established via this mechanism.

8. Conclusions

The program has successfully examined the performance of the HUWI equipment. The mathematical models provide useful quantitative data on the propagation of light in water. The performance of an active underwater imaging system is dependent on the properties of the water in which it operates. Underwater imaging systems operate in water of highly variable quality, with total attenuation coefficients typically in the range 0.07 (clear ocean) up to about 5 (very turbid estuary), with wide variation in the ratio of the component absorption and scattering coefficients. Signal levels can vary over many orders of magnitude, with the ratio of backscatter to target signal varying widely. The models provide signal predictions based on a knowledge of the optical properties of the water, the characteristics of the imaging equipment, the characteristics of the target and the system geometry. The model results provide a useful basis for establishing imaging system performance.

The radiometric data collected in the tank experiments and the observed imaging performance of the HUWI equipment provide evidence of the validity of the modelling process. The variations between measured and modelled results can be attributed to a number of factors. Measurement difficulties in the tank, calibration errors with the radiometers when measuring short laser pulses and difficulty in

accurately determining the optical properties of the water all contribute to the error budget.

The maximum range and resolution performance of HUWI were well represented by the mathematical modelling providing simple measurements of total attenuation and absorption were made. Comparisons made by measuring the radiation field scattered forward away from HUWI and back from a variety of ranges to HUWI support this result. Measurements made of these fields by the radiometers employed and by using the HUWI imager itself support this result.

The results indicate that the performance of any range-gated imaging system may be predicted for a particular optical set-up and for known values of the water optical properties. The mathematical model can also be used to model the performance of any imaging system with artificial illumination. By adding a module to compute natural lighting on the "target" this model could be extended to the natural lighting case.

9. References

1. Jones C. D., Bowcock C "Implementation of an Underwater Laser Range-gated Imaging System" DSTO-TN-0008
2. Koerber B.W., Wilsen P.J. "Analysis of Measurements of Laser Light Propagation in Sea Water at Jervis Bay" SRL-0120-RE.
3. Koerber B.W. "Mathematical Modelling of Optical Image Propagation in Water" DSTO-TR-0155
4. Adams T., Wilsen P.J., Koerber B.W "Performance of an Underwater Laser Range-gated Imaging System" DSTO-TR-0157
5. Duntley J "Light in the Sea" J. Opt. Soc Am 1963 vol 53 p214
6. Hodara Henri "Experimental results of small angle scattering" Agard LS-61 p 3-4.2

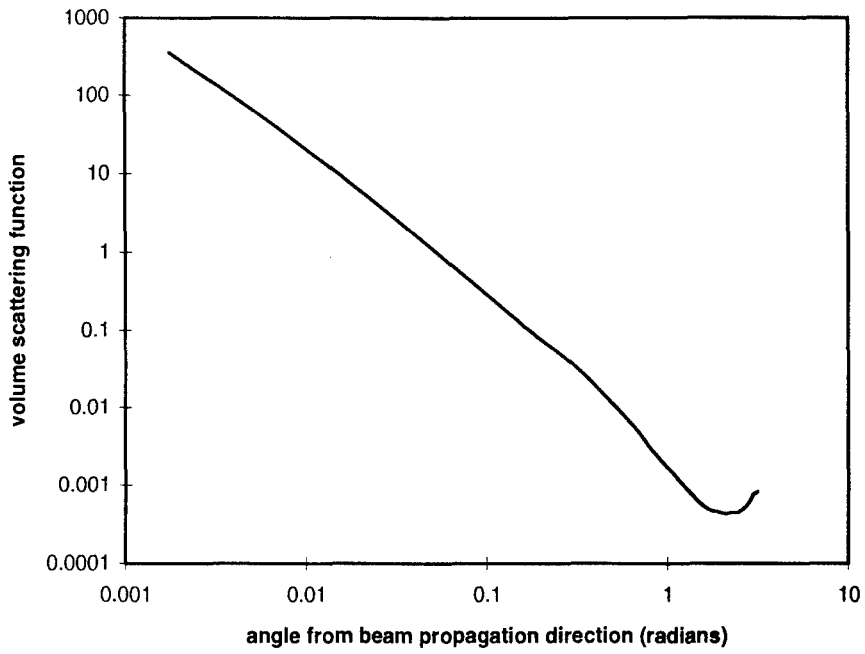


Figure 1 Volume Scattering function

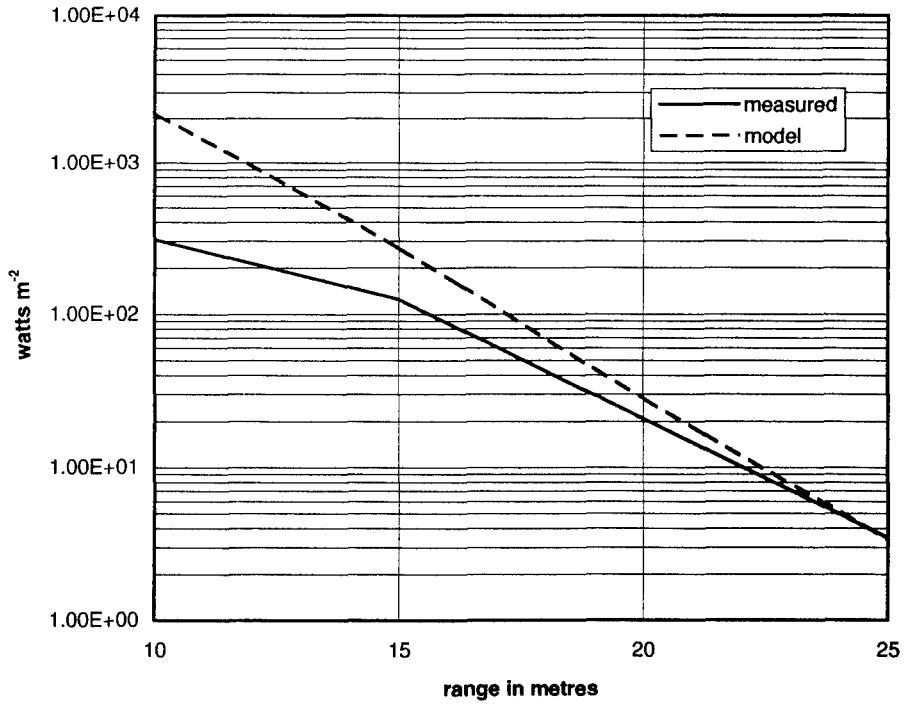


Figure 2 Radiometer 1 at 0 degrees Transmitter Narrow FOV

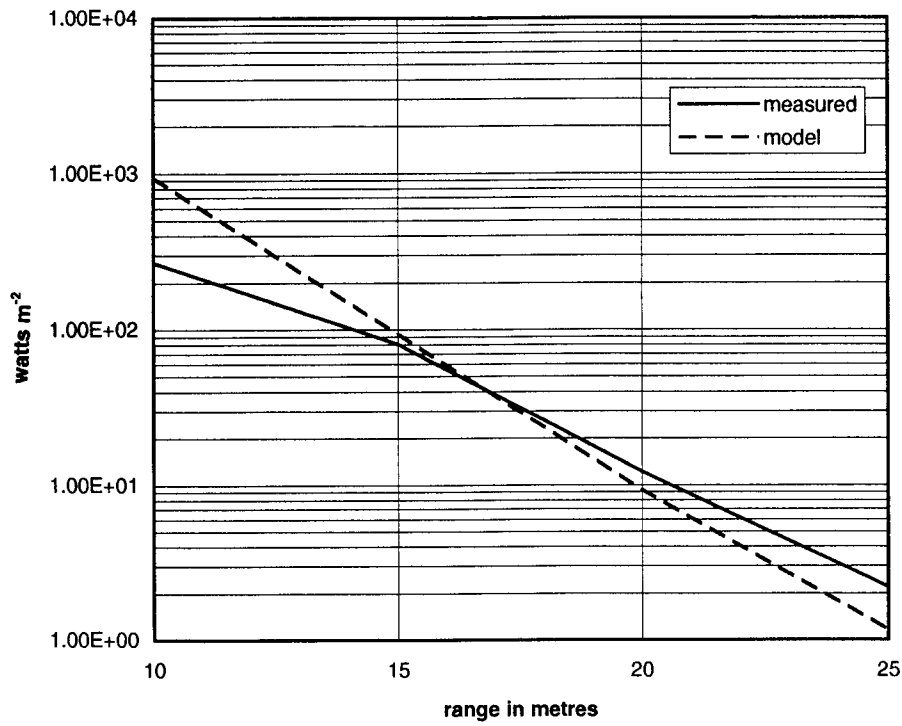


Figure 3 Radiometer 1 at 40 degrees Transmitter Narrow FOV

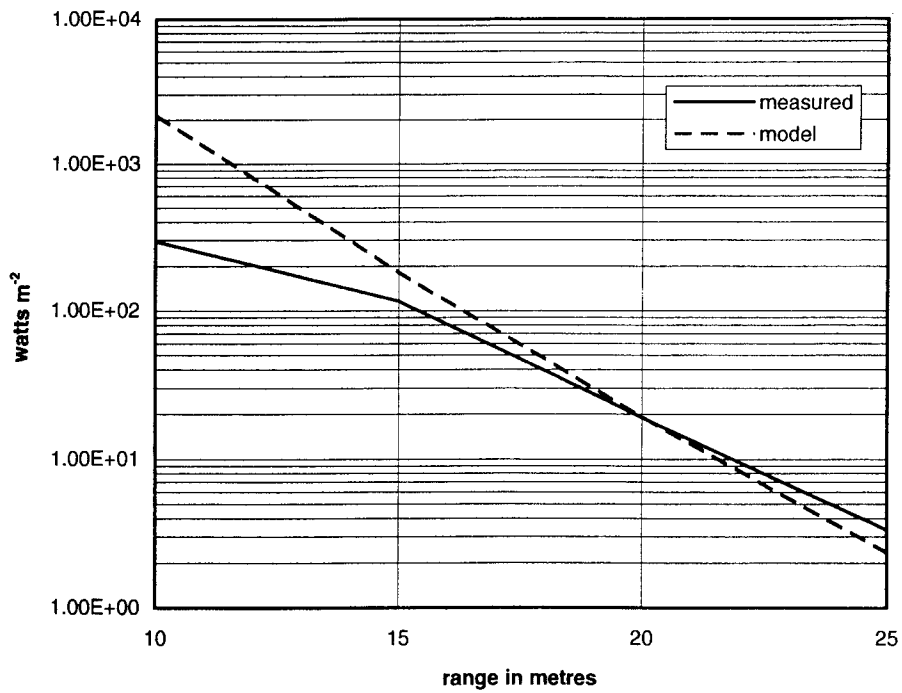


Figure 4 Radiometer 1 at 0 degrees Transmitter Wide FOV

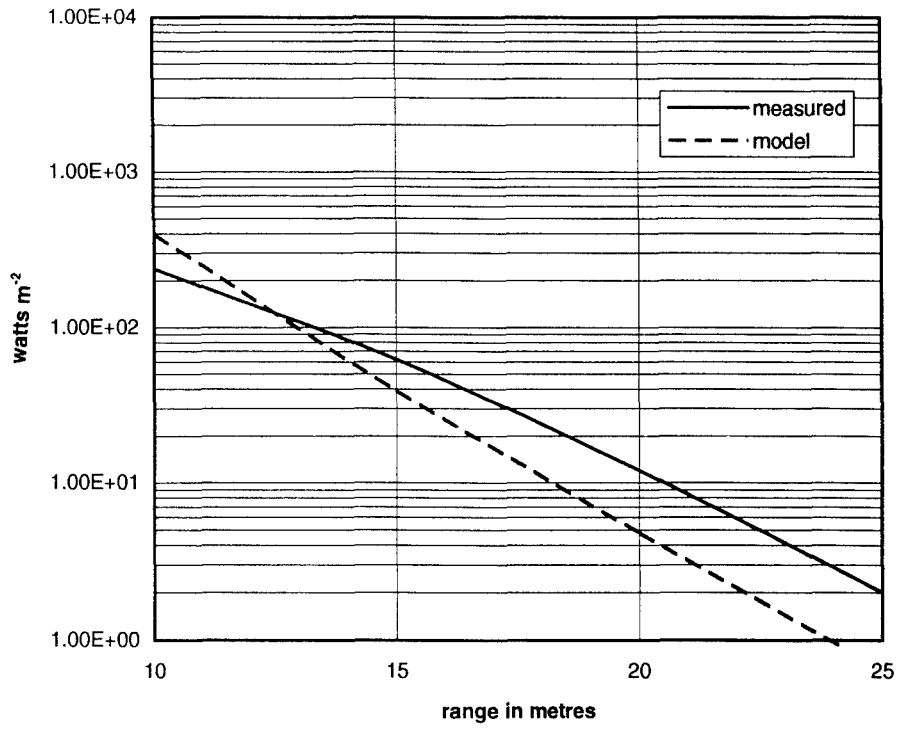


Figure 5 Radiometer 1 at 40 degrees Transmitter Wide FOV

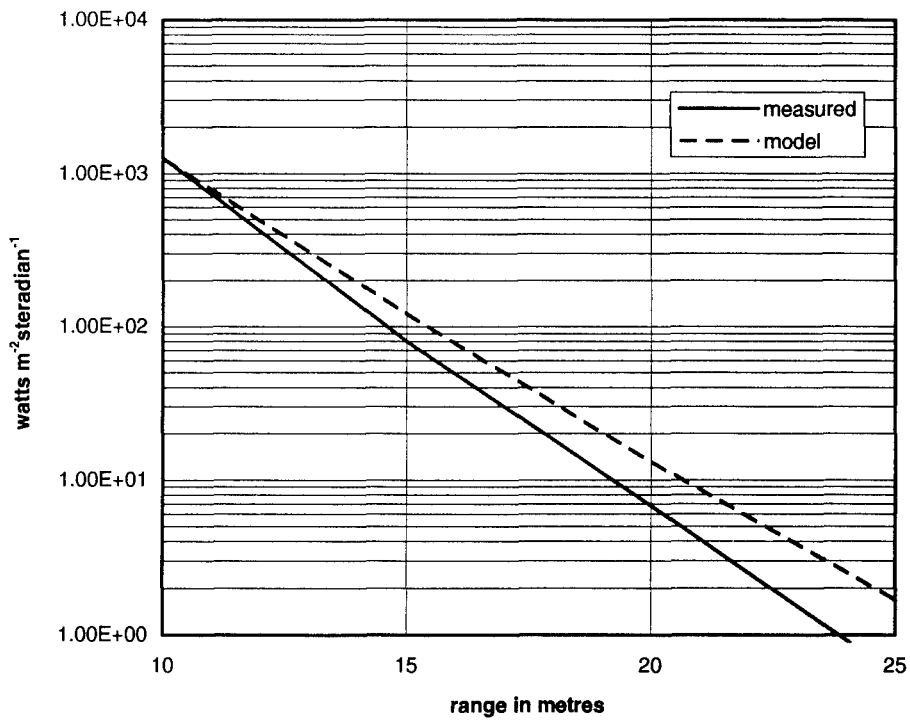


Figure 6 Radiometer 2 at 0 degrees Transmitter Narrow FOV

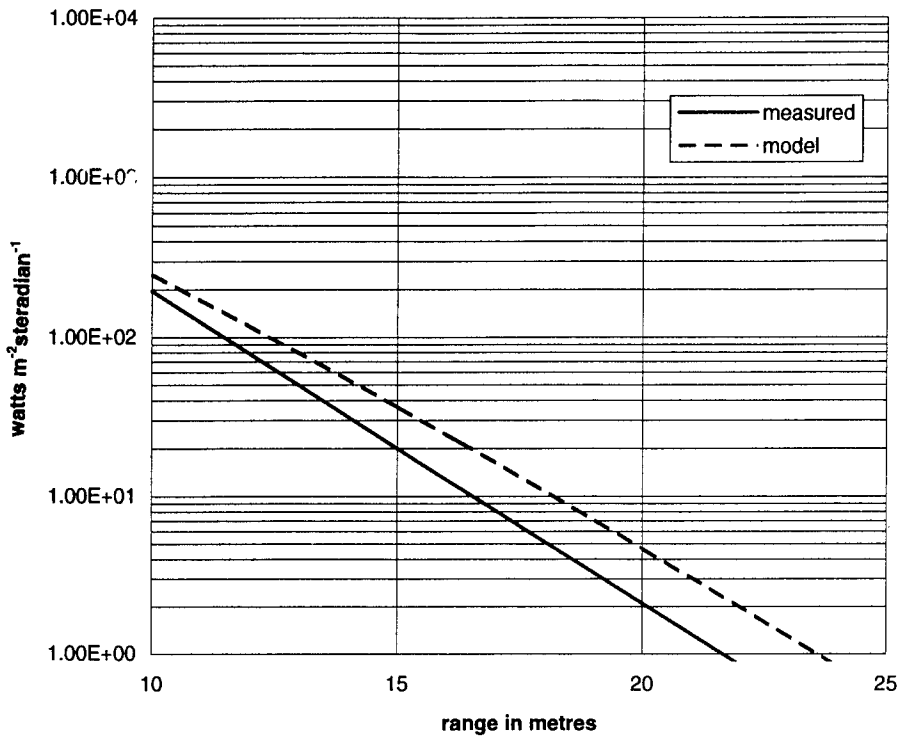


Figure 7 Radiometer 2 at 40 degrees Transmitter Narrow FOV

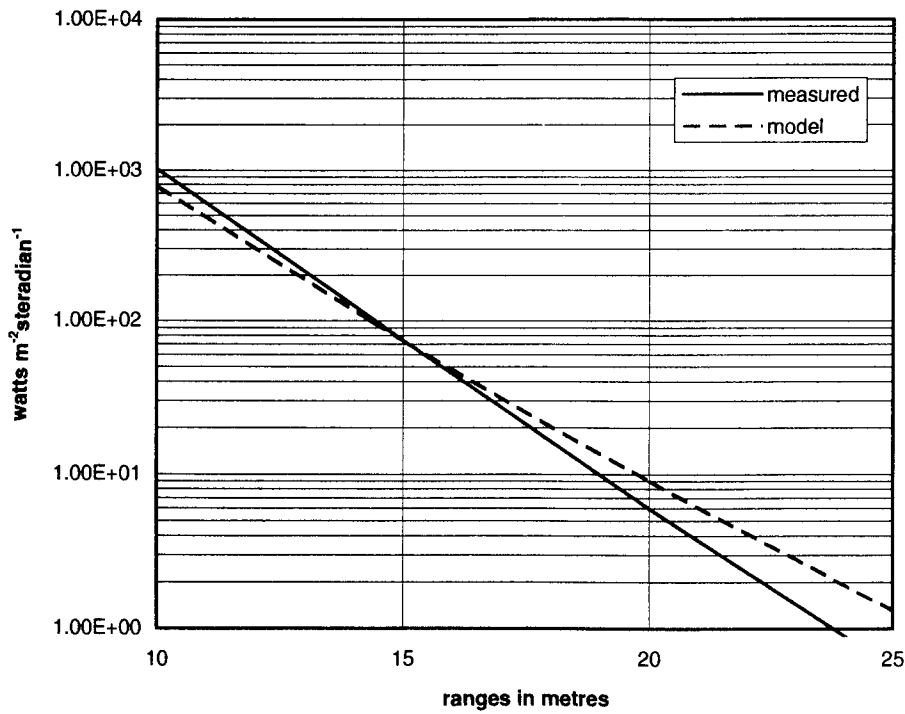


Figure 8 Radiometer 2 at 0 degrees Transmitter Wide FOV

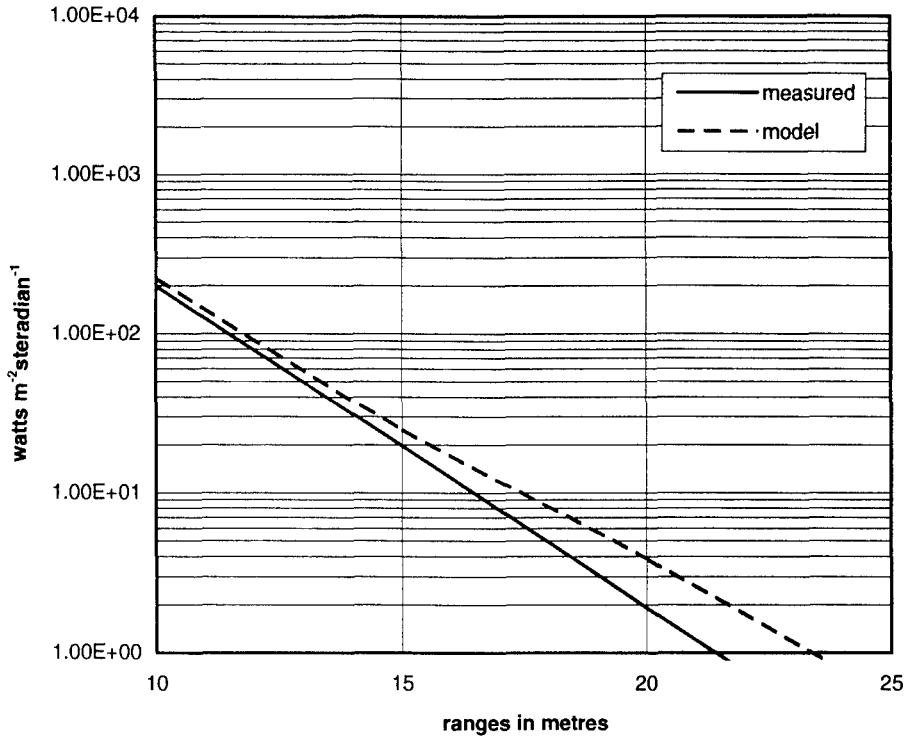


Figure 9 Radiometer 2 at 40 degrees Transmitter Wide FOV

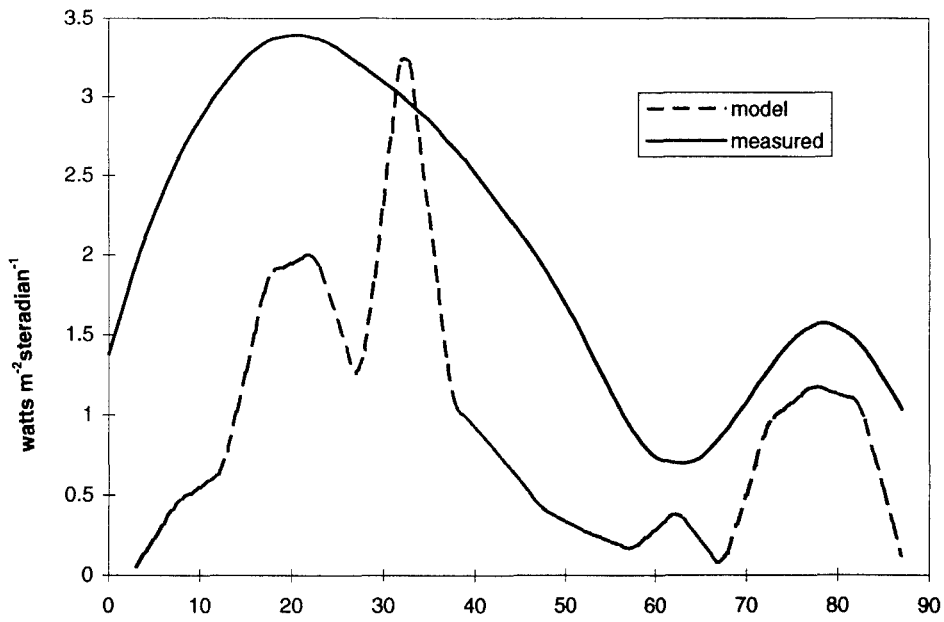


Figure 10 Radiometer 3 Target Range 8.5 metres

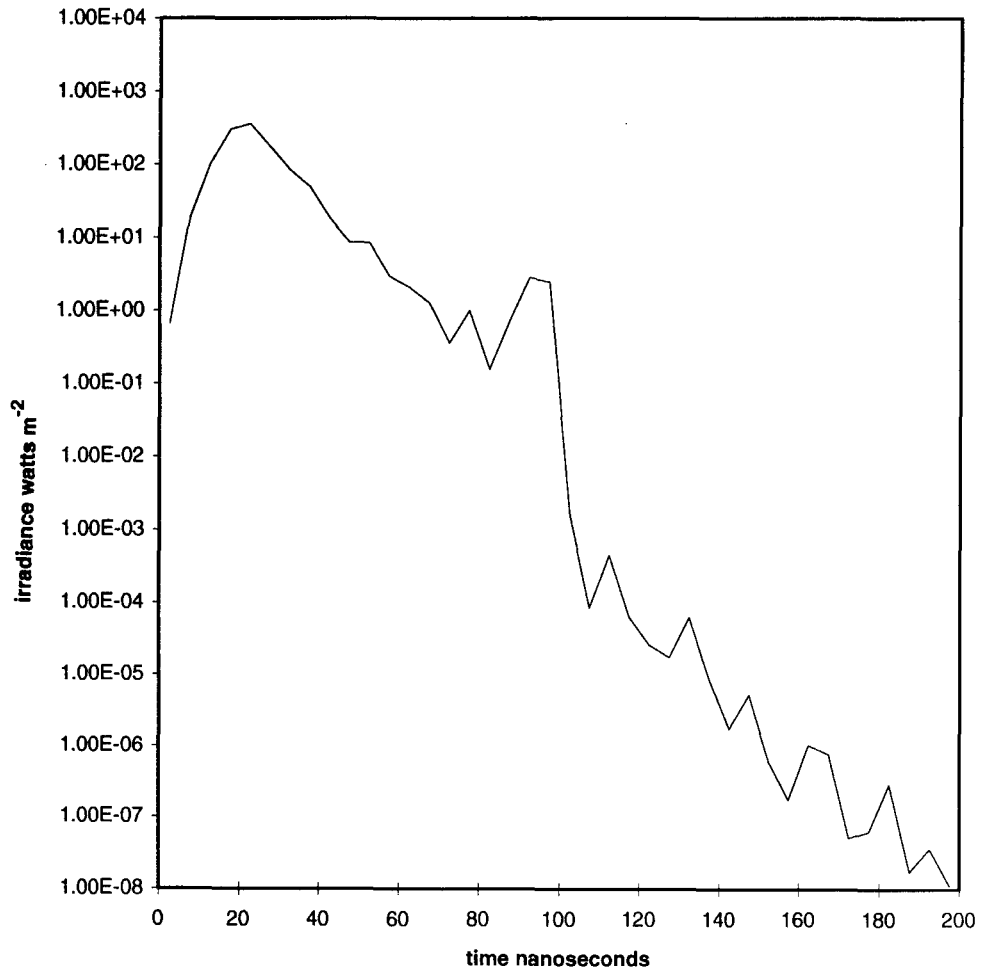


Figure 11 Target and backscatter signals for $c=0.6 \text{ m}^{-1}$ seen by HUWI

Optical Propagation Effects of an Underwater Laser Range-gated Imaging System

B.W. Koerber, T. Adams and P.J. Wilsen

(DSTO-TR-0156)

DISTRIBUTION LIST

TASK SPONSOR: DSMPW

1 copy

DEFENCE ORGANISATION

Defence Science and Technology Organisation

Chief Defence Scientist

FAS Science Policy

AS Science Corporate Management

Counsellor, Defence Science, London

Counsellor, Defence Science, Washington

Director General Scientific Advisers and Trials

Scientific Adviser POLCOM

Navy Scientific Adviser

Army Scientific Adviser

Airforce Scientific Adviser

Director Trials

} 1 shared copy

} Doc data sheet only

} Doc data sheet only

} 1 shared copy

} Doc data sheet only

} Doc data sheet only

} Doc data sheet only

Electronics and Surveillance Research Laboratory

Director

Chief Land Space and Optoelectronics Division

Research Leader Optoelectronics

Head Systems Integration

M. Brennan

R. Abbot

Spares

6 copies

Aeronautical and Maritime Research Laboratory

Director

Authors

T. Adams

P.J. Wilsen

DSTO Library

Main Library DSTOS

Library Fishermens Bend

2 copies

Library Maribyrnong
Library, MOD Pyrmont
Australian Archives

Doc data sheet only

Defence Central

OIC TRS, Defence Central Library
Officer in Charge, Document Exchange Centre
Defence Intelligence Organisation
Library, Defence Signals Directorate

7 copies

Doc data sheet only

Air Force

Director General Force Development (Air)

Doc data sheet only

Army

Director General Force Development(Land)

Doc data sheet only

Navy

Director General Force Development(Sea)
SO (Science), Director of Naval Warfare, Maritime
Headquarters
Annex, Garden Island, NSW 2000
RANTEWSS
Hydrographer

Doc data sheet only

Department of Defence

DOCUMENT CONTROL DATA SHEET

1. Page Classification Unclassified
2. Privacy Marking/Caveat (of document)

3a. AR Number AR-008-530	3b. Laboratory Number DSTO-TR-0156	3c. Type of Report Technical report	4. Task Number NAV95/037	
5. Document Date May 1996	6. Cost Code 821921	7. Security Classification Unclassified	8. No of Pages 18	
10. Title Optical Propagation Effects of an Underwater Laser Range-gated Imaging System		<input type="checkbox"/> L <input type="checkbox"/> U <input type="checkbox"/> U Document Title Abstract S (Secret) C (Conf) R (Rest) U (Unclas) * For UNCLASSIFIED docs with a secondary distribution LIMITATION, use (L) in document box.		
		9. No of Refs 6		
11. Author(s) B.W. Koerber, T. Adams and P. J. Wilsen		12. Downgrading/Delimiting Instructions Review in May 1999		
13a. Corporate Author and Address Electronics & Surveillance Research Laboratory PO Box 1500, Salisbury SA 5108		14. Officer/Position responsible for Security: Downgrading: Approval for Release:CLSOD.		
13b. Task Sponsor NAVY				
15. Secondary Release Statement of this Document Distribution additional to the initial list is limited to qualified officers of the Defence Department and the Defence Community of Australia, UK, USA, Canada and New Zealand. Other requests should be referred to Chief, Land, Space and Optoelectronics Division Electronics and Surveillance Research Laboratory.				
16a. Deliberate Announcement No Limitation				
16b. Casual Announcement (for citation in other documents) <input checked="" type="checkbox"/> No Limitation <input type="checkbox"/> Ref. by Author, Doc No. and date only				
17. DEFTTEST Descriptors Propagation, Range gating, Imaging systems, Underwater, Laser, Images, Forward scattering, Backscattering, Mathematical models			18. DISCAT Subject Codes	
19. Abstract A report on the verification of a suite of mathematical models related to propagation of light in water. The developed models were assessed by comparison with experimental results for forward scattering and backscattering, in addition to image propagation, using the high performance underwater imaging system.				

Reference: R9607/7/9 Pt3 Folio No. 41
Contact: Natalie Mahlkecht
E-mail: natalie.mahlkecht@dsto.defence.gov.au

Telephone: (08) 8259 6255

Facsimile: (08) 8259 6803

27th January 2000

To All Copyholders
cc: To the Team Leader of Records & Archives

AD-B222555

Notification of Downgrading/ Delimiting of DSTO Report

Please note that the Release Authority has authorised the downgrading/ delimiting of the report detailed here:

DSTO NUMBER	DSTO-TR-0156
AR NUMBER	AR-008-530
FILE NUMBER	UNKNOWN
REVISED CLASSIFICATION / RELEASE LIMITATION	UNCLASSIFIED Approved for Public Release

Please amend your records and make changes to your copy of the report itself to reflect the new classification/ release limitation.



Natalie Mahlkecht
Reports Distribution Officer
DSTO Research Library, Salisbury

*Received 5 June 2000
Annexed 5 June 2000*